Available on CMS information server

CMS CR -2024/353

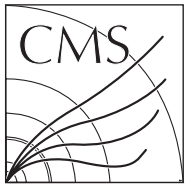

The Compact Muon Solenoid Experiment

Conference Report

Mailing address: CMS CERN, CH-1211 GENEVA 23, Switzerland

23 December 2024 (v4, 14 January 2025)

Searches for long-lived particles at the LHC

Lisa Benato on behalf of the ATLAS, CMS, and LHCb collaborations

Abstract

Recent results of searches for long-lived particles at the LHC experiments are presented. The focus of this report is on long decay lengths, beyond 1 m. These searches are performed by exploiting calorimeters and muon systems to their full capability. New Run 3 developments at the LHC experiments and new ideas for upcoming future dedicated experiments are discussed.

Presented at *Blois2024 35th Rencontres de Blois on Particle Physics and Cosmology*

Searches for long-lived particles at the LHC

Lisa Benato on behalf of the ATLAS, CMS, and LHCb collaborations
Institute for High Energy Physics, Austrian Academy of Sciences
Dominikanerbastei 16, 1010 Vienna, Austria
lisa.benato@oeaw.ac.at

Recent results of searches for long-lived particles at the LHC experiments are presented. The focus of this report is on long decay lengths, beyond 1 m. These searches are performed by exploiting calorimeters and muon systems to their full capability. New Run 3 developments at the LHC experiments and new ideas for upcoming future dedicated experiments are discussed.

1 Long-lived particles searches at the LHC

The Standard Model (SM) does not yet describe all the experimental evidences about the nature of matter and its interactions. Extensions of the SM predict new particles that are long-lived [1] if their couplings to the SM are small; if the available phase-space is suppressed; if they are produced through highly virtual intermediate states. Some examples of such extensions are: supersymmetric partners of the SM particles (SUSY), that can provide dark matter candidates; dark sectors communicating with the SM via the Higgs boson or dark photons portals, that can solve the Higgs boson mass hierarchy problem; axion-like particles (ALPs), that address the strong CP problem.

The long-lived particles (LLPs) search program at the LHC is very broad. LLP searches are challenging, because the LHC main detectors are not designed to capture these signatures; but they give unique opportunities for research and development, since new ideas can be applied at any level (reconstruction, trigger, analysis techniques). LLP searches require a non-standard use of the detector; they make use of non-standard data formats; and they are characterized by non-standard backgrounds. On the other hand, LLPs constitute a large, unexplored phase-space: new physics may have already been collected in LHC data.

In this conference report, some recent results on LLP searches performed by the ATLAS, CMS, LHCb collaborations are presented. Data are collected from LHC proton-proton collisions at 13 TeV (during the so-called Run 2 in 2016-2018), and at 13.6 TeV (Run 3: 2022-2025). This report will focus on long decay lengths: namely, LLP searches performed with calorimeters and with muon systems are discussed. New Run 3 developments at the LHC experiments and new ideas for upcoming future dedicated experiments are presented.

A more detailed description of the ATLAS, CMS, and LHCb experiments can be found in [2,3,4,5,6,7].

2 LLP searches with calorimeters

2.1 CMS: search for trackless and out-of-time jets

Pair produced SUSY neutralinos $\tilde{\chi}$ [8] are allowed to be long-lived and can travel significant distances ($\mathcal{O}(1)$ m) before decaying to a gravitino ($\tilde{G}$) and a Z or Higgs boson H, which in turn decay to hadrons. The $\tilde{G}$ is assumed to be the lightest SUSY particle, and hence a dark matter candidate; it is stable and hence it creates missing transverse momentum p_T^{miss} that can be used to trigger the data event acquisition. Given the long decay path of the $\tilde{\chi}$, its hadronic decay products will originate in the outer tracker and in the electromagnetic calorimeter (ECAL) of the CMS detector. In this search [9], the $H(Z)$ decay to hadrons will therefore be reconstructed as a jet characterized by two features: (a) since the CMS tracking efficiency decreases with displacement, such a jet will appear as nearly trackless; (b) a path length increase due to displacement, or a slow moving LLP, will make the jet appear as delayed with regards to the proton-proton interaction vertex; such a delay can be measured by the ECAL scintillating crystals. These two features are combined in a deep neural network (DNN) tagger, that uses as inputs the properties of the ECAL crystals and tracks associated to the signal jet. The signal region (SR) is defined when at least two jets have a large DNN score. The DNN response and the DNN inputs are studied in data; Monte Carlo (MC) samples are corrected accordingly. Two main sources of background contribute to the SR. (a) *Collision backgrounds*, consisting of prompt jets misidentified as trackless and delayed. The misidentification rate is evaluated in data control regions and the background yield is predicted with the matrix method. (b) *Noncollision backgrounds*, consisting of cosmic muons and beam induced backgrounds (BIB) creating ECAL deposits without associated tracks. Dedicated vetoes are designed to reject this contribution. The background rejection is such that 0.23 ± 0.10 events are expected in the SR; 0 events are observed. Limits on the $\tilde{\chi}$ production cross-section are set at 1 fb level for $m_\chi > 550$ GeV. A neutralino with a proper decay length of $c\tau = 0.5$ m is excluded up to a mass range of $m_\chi = 1.18$ TeV (Fig. 1, left).

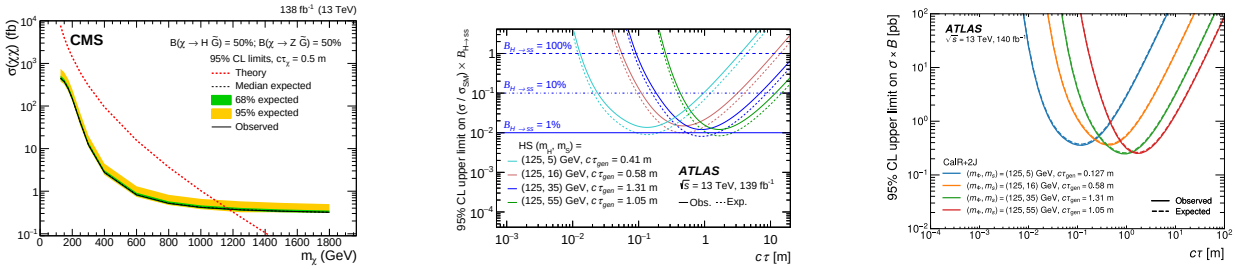

Figure 1 – Left: 95% CL expected and observed upper limits on neutralino $\tilde{\chi}$ pair production cross-section as a function of its mass when $c\tau = 0.5$ m [9]. Center: 95% CL expected and observed upper limits on the branching ratio of SM Higgs decay to a pair of LLPs as a function of $c\tau$, considering different mass hypotheses for the LLP candidate [11]. Right: 95% CL expected and observed upper limits on cross-section times branching ratio of a SM Higgs decay to a pair of LLPs as a function of $c\tau$, considering different mass hypotheses for the LLP candidate [12].

2.2 ATLAS: search for displaced hadronic jets in the calorimeter

Models predicting pair produced LLPs in exotic Higgs boson decays [10] consider the LLP lifetime as a free parameter. A dedicated search strategy has been developed by exploting the ATLAS hadronic calorimeter (HCAL) [11]. If a LLP decays to hadrons nearby the HCAL surface, it will generate a trackless jet with a low energy fraction in the ECAL compared to the energy deposits in the HCAL. This variable relating ECAL versus HCAL energies, named "CalRatio", has been implemented at trigger level to collect data in two different regimes, targeting respectively LLP masses below and above 200 GeV. This approach allows to access lower LLP masses compared to the CMS search described in Sec. 2.1. Analogously to [9], the background consists of either multijets produced by the strong interaction with mis-reconstructed tracks or neutral hadron abundance, or

of noncollision backgrounds (BIB and cosmic muons). A DNN tagger uses as input variables the features of tracks, of the calorimeter deposits and of the muon segments associated to a jet. An adversarial network mitigates the effects of MC mis-modelling, mostly found in the calorimeter cluster timing variable. A further event level BDT is trained by considering the 2 jets, triggered by the CalRatio trigger, with the largest DNN scores. A data-driven background estimation is performed by using the ABCD method. Limits are set for the production cross-section of the process $H \to SS \to 4f$ (f refers to fermions), considering the SM $m_H = 125$ GeV and larger m_H hypotheses. Branching ratios (BRs) of $\mathcal{O}(10)\%$ are excluded for a large range of S decay lengths, 20 mm $< c\tau <$ 10 m (Fig. 1, center).

A new result [12] targets pair produced LLPs in the so-called "merged + resolved" topology: one LLP is reconstructed as 1 CalRatio jet (used also for triggering the event), and the second is reconstructed as 2 resolved trackless jets. A per-event DNN variable is built such to be fully decorrelated with a variable measuring the degree of trackless-ness of the jets (namely, the angular distribution of tracks inside a jet). This approach (ABCDisco method [13]), in synergy with the exploitation of additional jet information, allows to improve the exclusion limits by three times (Fig. 1, right) when compared to [11]. In [12], the Higgs boson associated production with a SM W or Z decaying to leptons is also considered, and it is used to probe additional signal models, such as low mass ALPs ($0.1 < m_{ALP} < 4$ GeV) and dark photons (with masses in the range $5 - 400$ GeV).

3 LLP searches with muon systems (MSs)

3.1 ATLAS: displaced vertices in the MS

The ATLAS MS consists of a big volume of gas detectors, shielded by calorimeters (that reduce the SM backgrounds), and with tracking capabilities. Searches for very displaced signatures rely on the muon region of interest (RoI) cluster trigger [14], that works at hardware level (L1) by forming a coincidence of hits, and at software level (or high level trigger, HLT) by forming a cluster of 3 or 4 L1 muon RoIs within a solid angle of 0.4 radians. The gas detectors installed in the barrel, the monitoring drift tubes (MDT), are organized in multilayers (ML), as shown in Fig. 2 (left). Single ML hits form segments (indicated as arrows), and segments from different MLs are paired to form tracklets [15]. A combination of tracklets (3 or 4) defines a MS vertex and its position in (η, φ).

In [16], decays of pair produced LLPs are reconstructed as 2 MS vertices that should match RoI clusters at HLT. The backgrounds consist of punch-through jets that shower beyond the calorimeters and leak into the MS, and noncollision events (electronic noise, cosmic muons, BIB); however they are strongly suppressed by the 2 MS vertices requirement. An event yield of 0.32 ± 0.05 is expected and 0 events are observed. This analysis excludes exotic Higgs boson decays $H \to SS \to 4f$ to BRs below 0.1%. BR $> 10\%$ are excluded for LLP decay lengths within a very large range, namely 4 cm $< c\tau <$ 72.4 m (Fig. 2, right).

3.2 CMS: muon detector showers (MDS)

CMS utilizes a complementary approach, given the different structure of the MS. In fact, the muon chambers in the CMS endcap (cathode strips chambers, CSCs) and barrel (drift tubes, DTs) alternate passive material (iron and steel). This design makes the CMS MS act as a sampling calorimeter: the decay products of a neutral LLP with sufficiently long decay path ($c\tau > 1$ m) can ionize the gas and develop a shower by generating a high multiplicity of hits, shown in Fig. 3 (left) as orange markers, that are clustered to form a muon detector shower (MDS). A MDS can reconstruct any LLP decay (except to muons) and has sensitivity to light particles ($\mathcal{O}(100)$ MeV), otherwise not distinguishable from the overwhelming background in the inner layers of the detector. Unlike ATLAS, no dedicated triggers were present during Run 2, hence missing transverse momentum p_T^{miss} has been used to collect events where one LLP decays beyond the detector. The very first CMS result made use of the CSCs only [17]; a second result [18] combines MDS identified in the DTs. Exclusive categories are defined based on the number of reconstructed MDS (1-CSC,

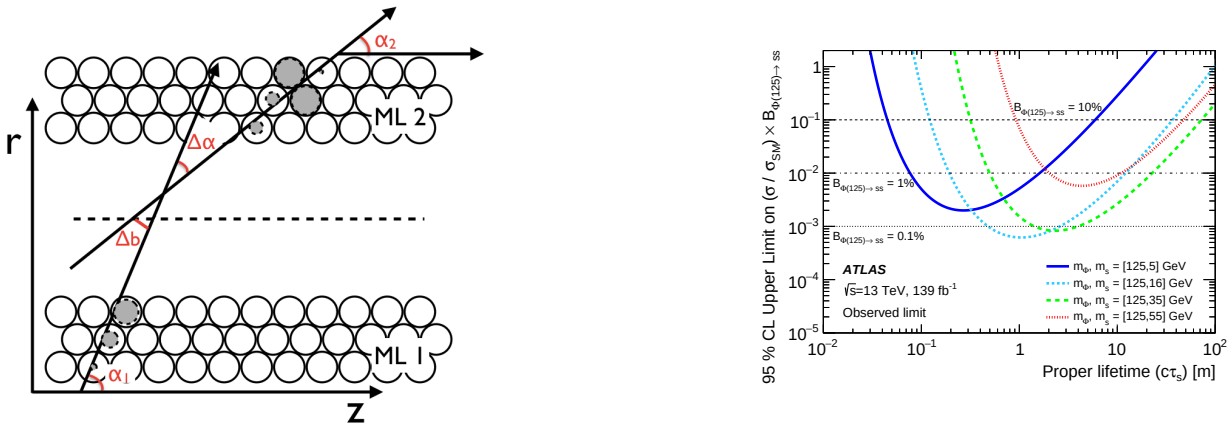

Figure 2 – Left: Schematic of a MDT chamber, displaying two ML segments forming a tracklet [15]. Right: 95% CL expected and observed upper limits on the BR of SM Higgs decay to a pair of LLPs as a function of $c\tau$, considering different mass hypotheses for the LLP candidate [16].

1-DT, 2-clusters); the background estimation is data-driven and uses the ABCD method. The ABCD plane is built for the 1-MDS category by using the number of hits in the MDS (the most discriminating variable) and the angular separation $\Delta\varphi$ between the MDS position and the p_T^{miss}. The ABCD plane for the 2-MDS category is built by using the number of hits in each cluster. The background composition is similar to that expected at ATLAS [16]; however, due to the larger amount of shielding material, CMS benefits from having a smaller background yield and therefore the 1-cluster category can be used to increase the discovery reach (while ATLAS [16] requires 2 MS vertices to sufficiently reject background).

In [18], 9 decay modes of the process $H \to SS$ are probed, including hadronic showers ($b\bar{b}$, $d\bar{d}$, K^+K^-, K^0K^0, $\pi^+\pi^-$), electromagnetic showers ($\pi^0\pi^0$, $\gamma\gamma$, e^+e^-), or both types ($\tau^+\tau^-$). As shown in Fig. 3 (right), the same sensitivity is achieved for the same shower type independent of the LLP mass. This search is sensitive to sub-GeV mass LLPs at BR = 0.1% level, and it sets the best limits to date on pair produced LLPs in exotic Higgs boson decays [10] in the range 0.04–0.40 m and above 5 m for $m_S = 15$ GeV; 0.3–0.9 m and above 3 m for $m_S = 40$ GeV, and above 0.9 m for $m_S = 55$ GeV. This search also sets the first limits obtained at LHC experiments to dark showers produced from Higgs boson decay [19].

A recent CMS result [20] reports a search for third generation vector-like leptons τ' decaying to a prompt SM τ lepton and a light pseudoscalar a_τ of mass 2 GeV, that is long-lived and decays to photons via a τ' loop. The displaced $a_\tau \to \gamma\gamma$ decay is reconstructed as an electromagnetic MDS, that tends to have a smaller spread and depth with regards to hadronic showers, since photons are more easily stopped by the passive material. The number of hits in the MDS is the main search variable, and its distribution is predicted from data events failing the prompt τ identification criteria. The background estimation is validated by considering MDS that are out-of-time compared to the proton-proton collisions. τ' masses are excluded up to 690 GeV. This is the first CMS search considering long-lived vector-like leptons.

3.3 LHCb: dark photons to dimuon

A search for dark photons decaying to a dimuon [21], $A' \to \mu^+\mu^-$, has been conducted with LHC Run 2 data collected by the LHCb experiment, corresponding to an integrated luminosity of 5.5 fb^{-1}. This analysis spans through an impressive range of the dark photon mass $m(A')$, and consists of both a prompt and a displaced search, covering 214 MeV $< m(A') <$ 70 GeV and 214 MeV $< m(A') <$ 250 MeV, respectively. The displaced analysis deploys a software trigger requiring dimuons forming a good quality displaced vertex to suppress prompt backgrounds. The backgrounds consist of: (a) photon conversions in the Vertex Locator detector (VELO), that are determined with a precise three-dimensional material map; (b) b-hadrons, that are reduced by

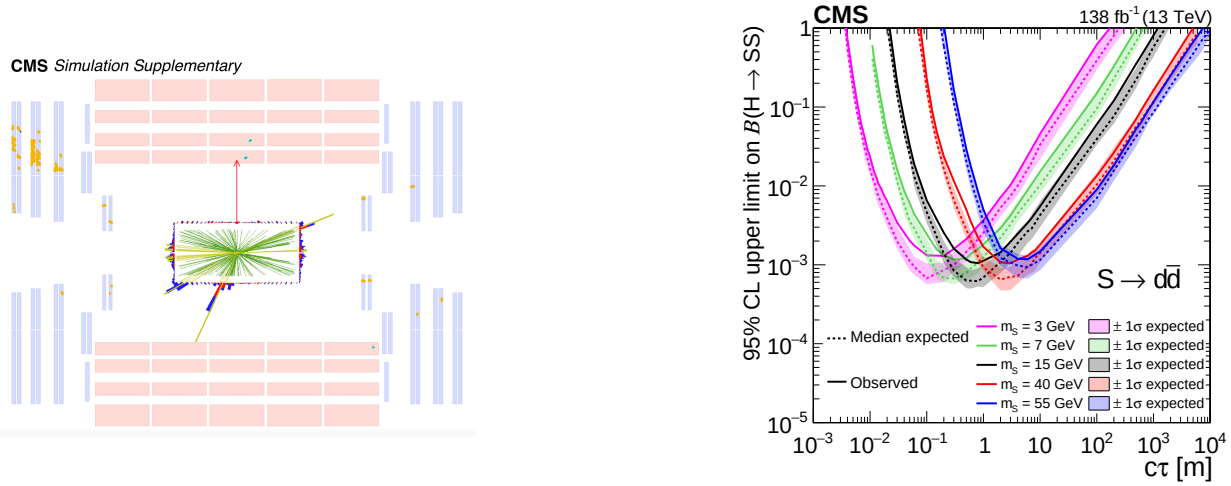

Figure 3 – Left: Event display of a simulated LLP signal event, producing a CSC hit cluster (orange markers) [17]. Right: 95% CL expected and observed upper limits on the BR of SM Higgs decay to a pair of LLPs as a function of $c\tau$, considering different mass hypotheses for the LLP candidate [18].

applying a BDT selection and vetoing on heavy-flavour induced muons at trigger level; (c) low mass tails of the $K^0_S \to \pi^+\pi^-$ decay, where π are misidentified as muons. The signal yield is evaluated from data, by resampling prompt, off-shell $\gamma^* \to \mu^+\mu^-$ events. No excesses are observed over the predicted background, and a large portion of the $[m(A'), \epsilon^2]$ plane is excluded (Fig. 4, left), where ϵ^2 describes the kinetic mixing of the A' to the SM photon, which is a parameter related to the A' lifetime.

It is also interesting to note there is an analogous CMS analysis searching for exotic Higgs boson decays to dark photons [22], $H \to A'A' \to \mu^+\mu^- X$, that uses a special CMS data stream called "scouting" [23], storing only a limited amount of event information but enabling looser trigger thresholds. This represents a clear case of complementarity across different LHC experiments.

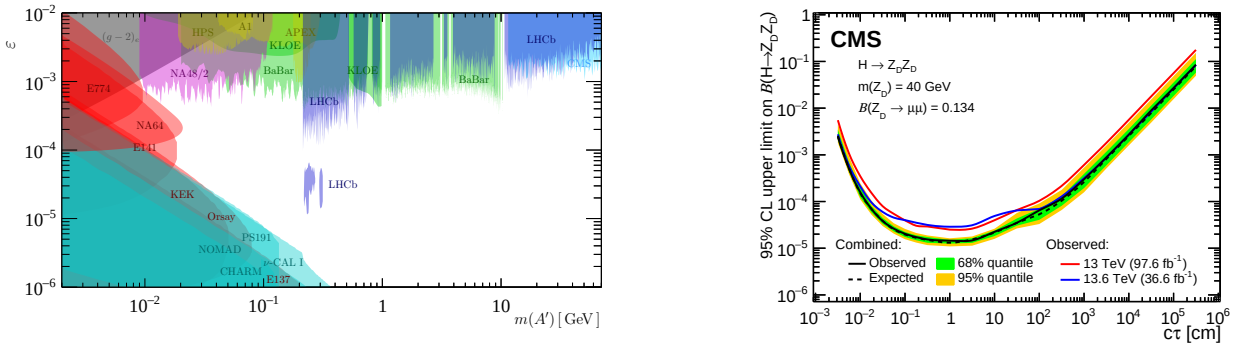

Figure 4 – Left: Comparison of the results in [21] to constraints from other experiments in the $[m(A'), \epsilon^2]$ plane. Right: 95% CL expected and observed upper limits on $H \to Z_D Z_D$ decay to a pair of displaced muons as a function of $c\tau$. The observed limits in Run 2 analysis, in Run 3 analysis and their combination are shown as blue, red, and black curves [24].

3.4 CMS: displaced dimuon with Run 3 data

The first CMS search performed with Run 3 data [24] probes the Hidden Abelian Higgs Model [25], in which the SM Higgs mixes with its dark sector counterpart, which decays to a pair of long-lived dark photons Z_D. The Z_D mixes with the SM Z and at least one is required to decay to displaced muons. This result superseeds the analogous Run 2 search [26]. The key development implemented for Run 3 is the trigger: new L1 algorithms correctly compute the momentum of muons produced in displaced vertices, rather than assuming they are produced nearby the proton collision point. Improved HLT algorithms recover efficiency for shorter muon tracks (a factor 2 when $c\tau(Z_D) \sim 1$

cm) and recover efficiency at larger displacement by discarding prompt muons (a factor 3 when $c\tau(Z_D) \sim 1$ m). The displaced dimuon candidates are reconstructed either as (a) global muons, by combining the MS with the tracker hits, which is the optimal strategy at lower displacement; or as (b) standalone muons, by using the MS only, which is the optimal strategy at larger displacement. The new Run 3 triggers allow to achieve a similar sensitivity with regards to the Run 2 analysis (97.6 fb^{-1}, red line in Fig. 4, right) by using only one third of the luminosity (collected during Run 3 in 2022 and corresponding to 36.6 fb^{-1}, blue line in Fig. 4, right).

4 LHC detectors developments for Run 3

4.1 ATLAS Run 3 upgrades

Several Run 3 upgrades of the ATLAS detector [3] impact LLP searches. The CalRatio search can benefit from (a) the upgraded ECAL LAr electronics, that provides finer granularity inputs to the trigger and allows a better control of rates, and hence a better resolution and rejection of pileup; (b) the extended coverage of the scintillator counter in the HCAL TileCal detector, making the system more robust against radiation. The MS vertices search can benefit from the installation of the new small wheel detectors in the endcap innermost stations. By taking advantage of new gas detector technologies (micro-mesh gaseous structure and small-strip thin gap chambers), it is possible to achieve faster triggers, higher precision tracking in the bending direction, and improved momentum resolution in the azimuthal coordinate, that allows to suppress more background.

At software level, the most impactful upgrade is the improvement of the large radius tracking, designed to deploy unused hits after the standard tracking algorithm to optimize the efficiency of reconstructing LLP decays in the range $5-300$ mm in the transverse coordinate and $200-500$ in the longitudinal one. While already deployed in Run 2 [27], the Run 3 version of the algorithm tightens several selections to reduce the fake rate and the pileup dependency. It has been commissioned studying K^0 displaced decays [28], achieving an excellent data-MC agreement, and it has already been deployed in a new Run 2 + Run 3 search for displaced leptons [29].

4.2 CMS Run 3 upgrades

The CMS HCAL readout granularity has been enhanced for Run 3 [5], to measure the hadronic showers depth in four different barrel layers. This upgrade allowed to design L1 trigger algorithms that identify HCAL trigger towers with significant energy deposits in higher depths, or pulses arriving at late times [30]. These new L1 triggers improve the efficiency to collect LLP hadronic decays nearby the HCAL surface ($\sim$ 3 m) up to a factor 3. This approach targets signatures analogous to those targeted by the ATLAS CalRatio algorithm, not covered at CMS so far.

ECAL timing properties have been implemented at HLT in Run 3 [30], improving the discovery reach for delayed and trackless jets (described in Sec. 2.1) to lower jet momentum, making CMS more competitive with regards to ATLAS.

A new L1 algorithm has been designed to collect MDS signatures at trigger level [30]. The algorithm counts the number of CSC hits in a chamber, which is required to be above a configurable threshold. This approach achieves a 20 times better signal efficiency when compared to the Run 2 unspecific trigger approach, based on p_T^{miss} (as described in Sec. 3.2).

4.3 LHCb Run 3 upgrades

The LHCb detector underwent significant Run 3 upgrades [7]. The most relevant for LLP searches are: (a) the silicon pixels of the VELO have been replaced and located closer to the beam; (b) a new high granularity upstream tracker (UT) has been installed immediately before the magnet; (c) three new scintillating fibre tracking stations (SciFi) have been installed downstream of the magnet. LHCb trigger is fully software as of Run 3: it consists of HLT1 running on GPUs and HLT2 running on CPUs, allowing a full detector readout at 40 MHz.

The LHCb tracking has been thoroughly studied for LLPs, considering the tracking detector upgrades. The standard approach, called *long tracks*, reconstructs tracks by using all the three tracking sub-detectors (VELO, UT and SciFi). *Downstream tracks* are reconstructed by matching hits in the UT and SciFi without using the VELO. *T-tracks* are built by using SciFi hits only. Using less sub-detectors and extrapolating over long distances where the magnetic field is lower poses several challenges, as these effects depauperate the momentum resolution and the vertex reconstruction efficiency, due to the higher likelihood of forming ghost vertices with spurious hits.

The potential capabilities of these different LLP tracking strategies have been studied considering a Higgs portal to dark matter model [31]: a light H', mixing with the SM H, can be produced in B decays and can decay to muons. The reconstructability of the decay vertex $H' \to \mu^+\mu^-$ is computed as a function of the H' mass and lifetime, by using long tracks, downstream tracks, and T-tracks. A large portion of phase-space can be explored by using these complementary approaches, when compared to the current HLT capabilities, that rely on long tracks only.

5 LLP-dedicated detectors at LHC

Several LLP-dedicated detectors are currently being designed or commissioned at the LHC, and planned to be operative during the High-Luminosity phase of the LHC (HL-LHC). A couple of dedicated detectors are currently collecting data which have already been used to publish world-leading results.

- *Transverse detectors* target LLPs in a very large mass range (from GeV to TeV) and can increase the lifetime coverage with regards to ATLAS, CMS, and LHCb.
  ANUBIS [32] is designed to be installed in the shaft of the ATLAS cavern. Its concept relies on the RPC technology developed for HL-ATLAS muon system. A detector prototype is currently being commissioned; the data acquisition is synchronized with ATLAS.
  CODEX-b [33] is designed to be a 10 m cube of RPC triplet modules, similarly to ANUBIS, and planned to be installed nearby LHCb. A smaller demonstrator of 2 m^3 is under commissioning with cosmic muons and its data acquisition is integrated with LHCb.
  MATHUSLA [34] is planned to be located on the surface of the CMS cavern. Its original massive design is being rescoped at a smaller size (40 m x 40 m x 17 m). A test stand comprising two layers of scintillator detectors is located above ATLAS and operating. A proposal for a small demonstrator of 10 m x 10 m is being evaluated and planned to be placed above CMS.

- *Forward detectors* target lighter LLPs (with masses below 1 GeV) that are more likely to be produced in the forward direction.
  FACET [35] is a detector proposal to be located 100 m from CMS. Its design will strongly rely on the CMS technology for the HL-LHC (high precision tracking, high granularity calorimeter) and possible detector configurations are under evaluation.
  MoEDAL-MAPP [36] operates since LHC Run1-2 (2010-2018): its Phase-0 (MoEDAL) consisted of a nuclear track detector (plastic array), a trapping detector array to capture highly ionizing particles, and a timepix array for real time radiation monitoring. The MoEDAL collaboration has published results of searches for monopoles [37] and dyons (particles with both electric and magnetic charges) [38]. The Phase-1 MAPP-1 upgrade as been deployed as of Run 3 in 2022 and it consists of 400 scintillator bars, to improve sensitivity to millicharged particles. The Phase-2 MAPP-2 upgrade will be deployed for the HL-LHC: the detector will be extended and will target LLPs decaying to charged particles and photons.
  FASER [39] is a running experiment designed to collect light and weakly-interacting particles. It is located 480 m from ATLAS in the forward direction. It consists of a large decay volume, tracking spectrometers and an electromagnetic calorimeter. FASER operates since the start of Run 3; the data collected so far have already been used to search for dark photons [40] and for ALPs [41]. In the former analysis, a search for dark photons produced in light meson decays,

that in turn decay to a pair of electrons, is conducted. Electron candidates are reconstructed in the tracking stations and calorimeters. The background consists of neutrinos and neutral hadrons. World-leading limits on dark photons with couplings ϵ^2 210^{-5}–110^{-4} and masses 17–70 MeV are set. The latter publication targets ALPs produced from photons (Primakoff effect) or mesons (B), that decay to a pair of photons. Photon candidates are reconstructed with the calorimeters and scintillation layers. The background consists of neutrinos from light quarks. World-leading limits on ALPs with masses up to 300 MeV and couplings to the SM W around 10^{-4} GeV^{-1} are set.

References

1. L. Lee, C. Ohm, A. Soffer, T.-T. Yu, *Prog. Part. Nucl. Phys.* **106**, 210-255 (2019).
2. ATLAS Collaboration, *JINST* **3**, S08003 (2008).
3. ATLAS Collaboration, *JINST* **19**, P05063 (2024).
4. CMS Collaboration, *JINST* **3**, S08004 (2008).
5. CMS Collaboration, *JINST* **19**, P05064 (2024).
6. LHCb Collaboration, *JINST* **3**, S08005 (2008).
7. LHCb Collaboration, *JINST* **19**, P05065 (2024).
8. S. Dimopoulos, M. Dine, S. Raby, S. Thomas, *Phys. Rev. Lett.* **76**, 3494-3497 (1996).
9. CMS Collaboration, *JHEP* **07**, 210 (2023).
10. M. J. Strassler, K. M. Zurek, *Phys. Lett.* B **651**, 374-379 (2007).
11. ATLAS Collaboration, *JHEP* **06**, 005 (2022).
12. ATLAS Collaboration, *JHEP* **11**, 036 (2024).
13. G. Kasieczka, B. Nachman, M. D. Schwartz, D. Shih, *Phys. Rev.* D **103**, 035021 (2021).
14. ATLAS Collaboration, *JINST* **8**, P07015 (2013).
15. ATLAS Collaboration, *JINST* **9**, P02001 (2014).
16. ATLAS Collaboration, *Phys. Rev.* D **106**, 032005 (2022).
17. CMS Collaboration, *Phys. Rev. Lett.* **127**, 261804 (2021).
18. CMS Collaboration, *Phys. Rev.* D **110**, 032007 (2024).
19. S. Knapen, J. Shelton, D. Xu, *Phys. Rev.* D **103**, 115013 (2021).
20. CMS Collaboration, http://cds.cern.ch/record/2905042, 2024.
21. LHCb Collaboration, *Phys. Rev. Lett.* **124**, 041801 (2020).
22. CMS Collaboration, *JHEP* **04**, 062 (2022).
23. CMS Collaboration, https://arxiv.org/abs/2403.16134.
24. CMS Collaboration, *JHEP* **05**, 047 (2024).
25. D. Curtin, R. Essig, S. Gori, J. Shelton, *JHEP* **02**, 157 (2015).
26. CMS Collaboration, *JHEP* **05**, 228 (2023).
27. ATLAS Collaboration, *Eur. Phys. J.* C **83**, (1081)2023.
28. ATLAS Collaboration, *JINST* **19**, P06029 (2024).
29. ATLAS Collaboration, https://arxiv.org/abs/2410.16835.
30. CMS Collaboration, https://cds.cern.ch/record/2865844, 2023.
31. L. Calefice et al., *Front. Big Data* **5**, (1008737)2022.
32. M. Bauer, O. Brandt, L. Lee, C. Ohm, https://arxiv.org/abs/1909.13022.
33. G. Aielli, E. Ben-Haim, R. Cardarelli et al., *Eur. Phys. J.* C **80**, (1177)2020.
34. D. Curtin et al., https://arxiv.org/abs/1806.07396.
35. S. Cerci et al., *JHEP* **06**, 110 (2022).
36. B. Acharya et al., *International Journal of Modern Physics* A **29**, (23-1430050)2014.
37. B. Acharya et al., *Phys. Rev. Lett.* **133**, 071803 (2024).
38. B. Acharya et al., *Phys. Rev. Lett.* **126**, 071801 (2021).
39. J. L. Feng, I. Galon, F. Kling, S. Trojanowski *Phys. Rev.* D **97**, 035001 (2018).
40. FASER Collaboration, *Phys. Lett.* B **848**, 138378 (2024).
41. FASER Collaboration, https://arxiv.org/abs/2410.10363.